



Review paper

## High-entropy perovskite ceramics: Advances in structure and properties

Yiwen Ding<sup>1,2</sup>, Keju Ren<sup>1,2</sup>, Chen Chen<sup>1,2</sup>, Li Huan<sup>1,2</sup>, Rongli Gao<sup>1,2,\*</sup>, Xiaoling Deng<sup>1,2,\*</sup>, Gang Chen<sup>1,2</sup>, Wei Cai<sup>1,2</sup>, Chunlin Fu<sup>1,2</sup>, Zhenhua Wang<sup>1,2</sup>, Xiang Lei<sup>1,2</sup>

<sup>1</sup>School of Metallurgy and Materials Engineering, Chongqing University of Science and Technology, Chongqing 401331, China

<sup>2</sup>Chongqing Key Laboratory of Nano/Micro Composite Materials and Devices, Chongqing 401331, China

Received 11 September 2023; Received in revised form 1 February 2024; Received in revised form 6 March 2024; Accepted 15 March 2024

### Abstract

High-entropy ceramic materials usually refer to the multi-principal solid solution formed by 5 or more ceramic components. Due to its novel “high-entropy effect” and excellent performance, it has become one of the research hotspots in the field of ceramics in recent years. As the research system of high-entropy ceramics has gradually expanded from the initial rock salt oxides (Mg-Ni-Co-Cu-Zn)O to fluorite oxides, perovskite oxides, spinel oxides, borides, carbides and silicates, its special mechanical, electrical, magnetic and energy storage properties have been continuously discovered. Based on the basic principle of high-entropy materials, this paper mainly introduces the prominent perovskite-type oxide high-entropy ceramics in recent years from the perspective of ceramic structure and properties, and predicts the development trend of high-entropy perovskite-type ceramics in the next few years.

**Keywords:** high-entropy ceramics, perovskite oxide, structure, properties

### I. Introduction

The development of dielectric ceramics began in the early 20<sup>th</sup> century and has become a critical type of material for manufacturing basic components in the electronics industry. It has been widely applied in various fields of production and daily life. In the past decade, with the rapid development of electronic components in related fields such as communication, household appliances, automobiles and military, the demand for dielectric ceramics has been continuously increasing, demonstrating significant market potential and strong economic benefits. To meet the ever-evolving needs of human society and the growing market demand, research institutes have conducted in-depth studies on dielectric ceramic materials, processes, equipment, and formulations. The research level of domestic dielectric ceram-

ics has been continuously improving, and the dielectric ceramics industry is showing a thriving development trend, with perovskite-type oxide ceramics being one of the outstanding performers.

Crystal structure of perovskite-type (ABO<sub>3</sub> structure) oxide ceramics is typically composed of a 12-coordinated A-site atom, a 6-coordinated B-site atom and an octahedral arrangement of oxygen atoms. Due to the higher coordination numbers of A and B sites, there are numerous combinations of different cations, leading to variations in the sizes of A and B site cation radii. This results in changes in the tolerance factor ( $t$ ), lattice distortions and a reduction in the symmetry of the perovskite structure. Consequently, perovskite ceramics exhibit diverse physical and chemical properties, which is promising for a wide range of applications in solar cells, photocatalysis, proton conductors, dielectric materials, ferroelectrics and multiferroics [1–9].

The earliest report on high-entropy materials was Prof. Junwei Ye's work on high-entropy alloys in 2004.

\*Corresponding author: tel: +86 13970784755, e-mail: gaorongli2008@163.com (R. Gao) dgxmd@163.com (X. Deng)

Since then, with the discovery of a series of high-entropy alloys, an understanding of high-entropy materials has deepened [10–14]. Entropy is a measure of the degree of disorder in a thermodynamic system. The Boltzmann relation  $S = k_B \cdot \ln \Omega$  (where  $k_B$  is the Boltzmann constant) expresses this relationship mathematically, where  $S$  represents the macroscopic system entropy, which is a measure of the degree of molecular motion or arrangement disorder.  $\Omega$  is the number of possible microscopic states. The Gibbs free energy formula,  $G = H - T \cdot S$ , is used to determine the stability of a system. The concept of entropy stability is based on the increase of the system's configuration entropy ( $S_{config}$ ), which reduces the Gibbs free energy  $G$  of the system and stabilizes the single-phase crystal structure. The high entropy ceramics lattice comprises two sublattices: the anion sublattice, which can accommodate anions and some vacancies, and the cation sublattice, which is randomly occupied by various metal atoms. The molar configurational entropy of system can be calculated by the following equation:

$$S_{config} = -R \left( \frac{X}{X+Y} \sum_{i=1}^N x_i \ln x_i + \frac{Y}{X+Y} \sum_{j=1}^N x_j \ln x_j \right) \quad (1)$$

$x_i$  and  $x_j$  represent the molar fraction of cations and anions, respectively,  $X$  and  $Y$  represent the lattice number of cations and anions, respectively,  $R$  is the molar gas constant (8.314J/(mol·K)). However, in oxide system only cation sublattice should be considered and corresponding equation will be simpler:

$$S_{config} = -R \frac{X}{X+Y} \sum_{i=1}^N x_i \ln x_i \quad (2)$$

For an equimolar system with five components the increase of configuration entropy ( $S_{config}$ ) is  $1.61R$ . In general, materials with  $S_{config} \geq 1.61R$  are classified as high-entropy materials, those with  $1.61R > S_{config} \geq 1R$  are classified as medium-entropy materials and materials with  $S_{config} < 1R$  are classified as low-entropy materials [15–18].

In 2015, Rost *et al.* [18] extended the definition of high-entropy materials to the inorganic non-metallic field. Their team chose a pentavalent cation-equivalent oxide system (Mg,Ni,Co,Cu,Zn)O and reported the synthesis of large-scale high-entropy oxides, which they named entropy-stabilized compounds.

As the first discovered high-entropy ceramics, the (Mg,Ni,Co,Cu,Zn)O system has not only provided new insights for the discovery of new materials, but also exhibits excellent properties together with its derivatives, making it highly promising in applications such as energy storage, catalysis, thermal and environmental protection. Subsequently, more high-entropy oxide ceramics with different structures have been explored. In recent years, research on high-entropy oxides has primarily focused on rock salt-type structures [20], among others. However, the significance of high-entropy perovskite oxide ceramics cannot be overlooked due to

their excellent structural stability and various outstanding physical properties.

High-entropy perovskite oxide ceramics, characterized by multiple components and equal elemental ratios, have exhibited a series of outstanding properties since their inception. These properties include high-temperature stability [21], high strength [22], high hardness [23], giant dielectric constant [24], excellent dielectric performance [25], catalytic performance [26], magnetic properties [27] and lithium ion storage performance [28,29]. Since 2015, there has been a rapid increase in research papers on high-entropy perovskite ceramics, with over hundred publications reported until 2022, covering diverse systems.

## II. Structure of perovskite high-entropy oxides

Various crystal structures have been confirmed for high-entropy perovskite oxide materials. The detailed phase formation mechanisms behind these structures vary significantly depending on the specific crystal structure, element combinations and compositions of the high-entropy perovskite oxide materials. However, due to the random distribution of metals in the cation sublattice, they all exhibit enhanced high-temperature stability, resulting in uniformly dispersed metal oxide solid solutions. The excellent stability of high-entropy perovskite oxides has contributed to the rapid development of this research field, particularly in electrochemical applications.

Preparation method of ceramics has a great influence on high-entropy perovskite ceramics. In recent years, many researchers have used different methods to prepare high-entropy perovskite ceramics with good performance. The earliest high-entropy ceramics were prepared by solid phase reaction method. First, raw materials were fully mixed by ball milling and partial solid solution occurs, and then the mixed raw materials were fully calcined at high temperature to form a uniform and single high-entropy phase. In order to prevent the dissolution, phase separation or second phase precipitation of the formed high-entropy phase during the cooling process, rapid cooling methods such as quenching were usually used for preparation, as shown in Fig. 1 [19]. Solid state reaction method is the most common method for preparing high-entropy ceramics because of its simple reaction principle, high yield and low equipment requirements. However, the solid state reaction method

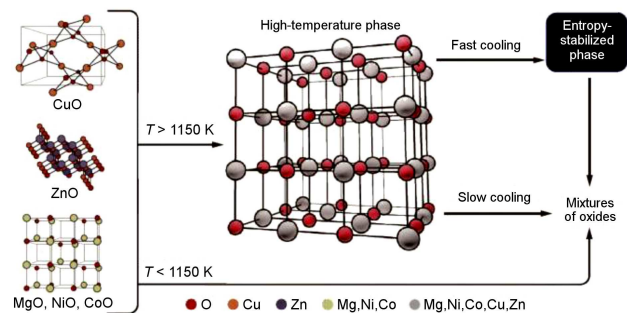


Figure 1. Structure of oxides and the phase transformation processes under different temperatures and heat treatment processes [19]

also has obvious shortcomings, for example, the reaction temperature is high, the reaction time is long, the product proportion is difficult to control accurately and impurities are easily introduced during the preparation process. Therefore, some researchers have developed different methods to synthesize high-entropy ceramics under relatively mild conditions starting from the precursor, such as sol-gel method, co-precipitation method, etc. Atomic-level mixing of raw materials is achieved, thus reducing the energy barrier required for the synthesis of high-entropy materials.

### 2.1. Titanate based high-entropy ceramics

The first generation of high-entropy perovskite ceramics is characterized by the same molar ratio of cations and a single-phase structure. Thus, Jiang *et al.* [30] synthesized different high-entropy oxides with perovskite structure and general formula  $A(\text{Zr}_{0.2}\text{Sn}_{0.2}\text{Ti}_{0.2}\text{Hf}_{0.2}\text{B}_{0.2})\text{O}_3$  where  $A = \text{Ba}, \text{Sr}$  and  $B = \text{Mn}, \text{Nb}, \text{Ce}, \text{Y}, \text{Nb}$  by solid state reaction. They analysed the conditions for the formation of high-entropy perovskite structures, considering tolerance factor, atomic size difference and mixing entropy. This study laid the groundwork for the research on high-entropy perovskite oxide ceramics. Building upon this, Biesuz *et al.* [31] investigated the effects of conventional and plasma sintering processes on the structure and properties of perovskite high-entropy  $\text{Sr}(\text{Zr}_{0.94}\text{Y}_{0.06})_{0.2}\text{Sn}_{0.2}\text{Ti}_{0.2}\text{Hf}_{0.2}\text{Mn}_{0.2}\text{O}_{3-x}$  ceramics.

Zhang *et al.* [32] prepared high-entropy perovskite type  $(\text{Ca}_{0.2}\text{Sr}_{0.2}\text{Ba}_{0.2}\text{La}_{0.2}\text{Pb}_{0.2})\text{TiO}_3$  ceramics with  $Pm\bar{3}m$  space group cubic structure by solid state reaction method. The high-entropy ceramics exhibit long-range structural order and short-range chemical disorder with widely distributed nanosize grains. The structural analyses also confirmed high-density and compacted structure with only a few macroscopic defects (Fig. 2).

The grains were well connected with the sharp edges, which is mainly due to the high activity of the lattice diffusion mechanism. With the sintering temperature increasing from 1200 to 1350 °C, the average grain size gradually increases from 0.6 to 2.3 μm and at 1350 °C some large grains appear (Fig. 2). The microstructure evolution is a combination of lattice diffusion and grain boundary diffusion, resulting in the element homogenization and densification of the perovskite structures.

Recently, Zhou *et al.* [6,25] prepared a series of high-entropy  $\text{Ba}(\text{Zr}_{0.2}\text{Ti}_{0.2}\text{Sn}_{0.2}\text{Hf}_{0.2}\text{Me}_{0.2})\text{O}_3$  ( $\text{Me} = \text{Y}^{3+}, \text{Nb}^{5+}, \text{Ta}^{5+}, \text{V}^{5+}, \text{Mo}^{6+}, \text{W}^{6+}$ ) ceramics with equal molar ratios at the B-site using the solid-state reaction method. Three types of multi-cation solid solutions formed pure phase compounds, while only two compounds were sintered into ceramics. Microstructural analysis revealed that configurational entropy had influence on the phase stability and grain growth. The tolerance factors of both ceramics ( $t = 1.03$ ) were higher than 1 (ideal value for cubic perovskite crystals), and the ceramics exhibited pure pseudocubic phase without any secondary phases. Among them,  $\text{BaSnO}_3$  showed the best match due to the closest proximity of the  $\text{Sn}^{4+}$  ion radius (0.64 Å) to the average radius (0.674 Å) of the B-site. Grain boundaries of both samples were clearly observed, and almost no porosity was observed throughout the samples, which corresponded to the calculated densities of 92 and 95 %TD, respectively. Additionally, the presence of small grain sizes indicated the extreme disorder within the grains formed after the mixing of the five cations at the B site, thereby suppressing grain growth.

### 2.2. Manganite based high-entropy ceramics

Sarkar *et al.* [33] successfully synthesized perovskite-type high-entropy ceramics with up to 10 constituent elements of transition metals and rare

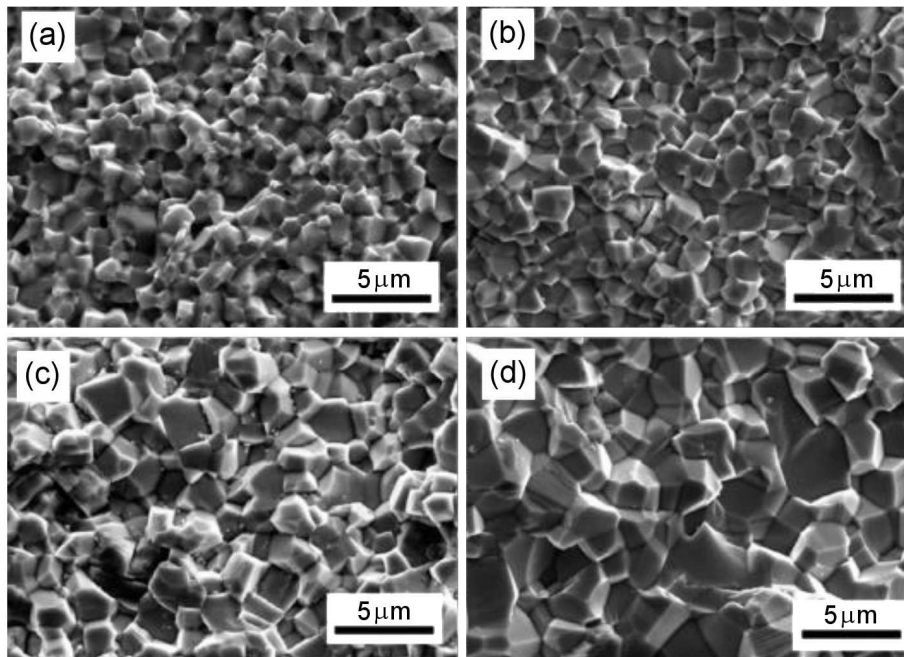


Figure 2. Cross sectional SEM micrographs of high-entropy  $(\text{Ca}_{0.2}\text{Sr}_{0.2}\text{Ba}_{0.2}\text{La}_{0.2}\text{Pb}_{0.2})\text{TiO}_3$  ceramics sintered at: a) 1200 °C, b) 1250 °C, c) 1300 °C and d) 1350 °C [32]

earth elements (Gd,La,Nd,Sm,Y)(Co,Cr,Fe,Mn,Ni)O<sub>3</sub>, demonstrating the reversible transition from multi-phase to single phase during cyclic thermal treatment, which strongly confirms the entropy-driven structural stabilization effect in the aforementioned perovskite systems.

Schweidler *et al.* [34] synthesized similar perovskite-type high-entropy materials (Gd<sub>0.2</sub>La<sub>0.2-x</sub>Sr<sub>x</sub>Nd<sub>0.2</sub>Sm<sub>0.2</sub>Y<sub>0.2</sub>)(Co<sub>0.2</sub>Cr<sub>0.2</sub>Fe<sub>0.2</sub>Mn<sub>0.2</sub>Ni<sub>0.2</sub>)O<sub>3</sub> ( $x = 0$  and 0.2) for the first time using mechanochemical synthesis and modified Pechini method. By comparing different synthesis methods, not only the compositional elements of high-entropy materials can be customized, but the synthesis methods can also be optimized according to the requirements in order to overcome the limitations of traditional ceramics.

### 2.3. (Bi<sub>0.5</sub>Na<sub>0.5</sub>)TiO<sub>3</sub> type of high-entropy ceramics

Zhou *et al.* [35] prepared perovskite (La<sub>0.5</sub>Li<sub>0.5</sub>)<sub>x</sub>[(Bi<sub>0.5</sub>Na<sub>0.5</sub>)<sub>0.25</sub>Ba<sub>0.25</sub>Sr<sub>0.25</sub>Ca<sub>0.25</sub>]<sub>1-x</sub>TiO<sub>3</sub> ceramics via a solid-state method. Surface scanning electron microscopy analysis of the high-entropy ceramics with varying compositions revealed a compact microstructure for each composition. All grains exhibited a cubic morphology, with their sizes gradually decreasing with an increase in the composition ratio until reaching a stable state. Sun *et al.* [36] prepared high-entropy ceramics with similar com-

position (Bi<sub>0.2</sub>Na<sub>0.2</sub>Ba<sub>0.2</sub>Ca<sub>0.2</sub>Sr<sub>0.2</sub>)TiO<sub>3</sub> by using a hydrothermal method. The average particle size of the synthesized powder was measured to be 40 nm (Fig. 3a), indicating that the multi-phase particles were mixed at the nanoscale, which is much smaller compared to the micrometer-sized powder obtained through traditional solid-state methods. These nanoscale particles promote a more uniform mixing during ceramic processing, leading to the improved chemical homogeneity and enhanced high-entropy effects. Thus, the high-entropy ceramics were obtained after sintering at 1180–1220 °C and exhibited excellent chemical homogeneity and a single tetragonal phase. SEM analyses demonstrated a dense microstructure with minimal presence of pores in the high-entropy ceramics (Fig. 3b). The chemical disorder in the A-site elements results in significant lattice distortion, effectively disrupting the symmetry of the TiO<sub>6</sub> octahedra and leading to dielectric relaxation. This phenomenon enhances the energy storage performance of high-entropy ceramics.

Ning *et al.* [37] fabricated ABO<sub>3</sub> structured high-entropy ceramics, (NaBaBi)<sub>x</sub>(SrCa)<sub>(1-3x)/2</sub>TiO<sub>3</sub> by traditional solid-state reaction and sintering at 1250–1300 °C. The ferroelectric and dielectric properties of non-stoichiometric high-entropy ceramics were investigated. It was found that all samples exhibited a dense and uniform microstructure without detectable porosity (Fig. 4). As the  $x$  content increased, the grain size grad-

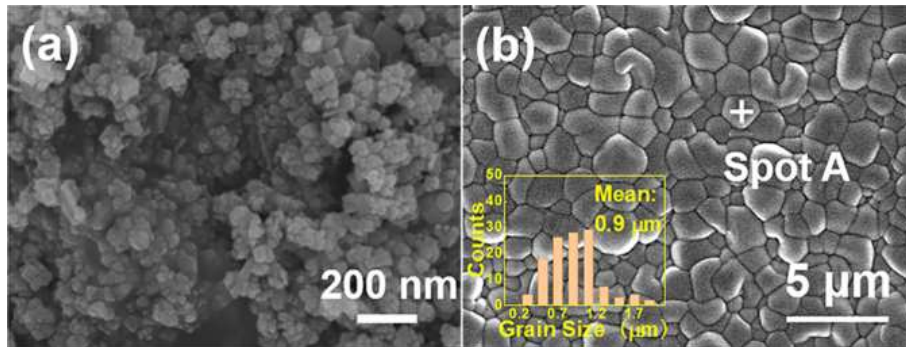


Figure 3. SEM images of high-entropy (Bi<sub>0.2</sub>Na<sub>0.2</sub>Ba<sub>0.2</sub>Ca<sub>0.2</sub>Sr<sub>0.2</sub>)TiO<sub>3</sub>: a) hydrothermally synthesized powder and b) ceramics sintered at 1200 °C [36]

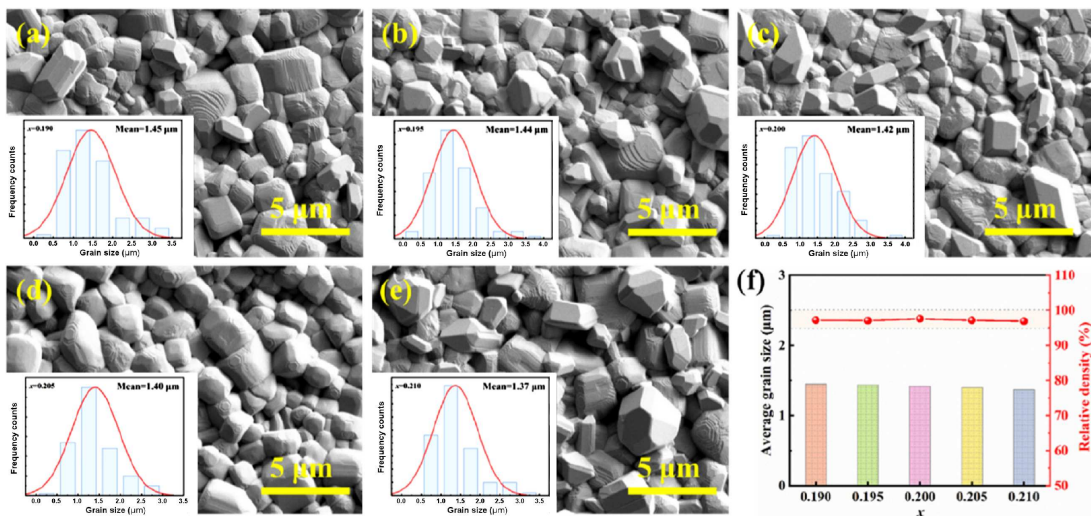
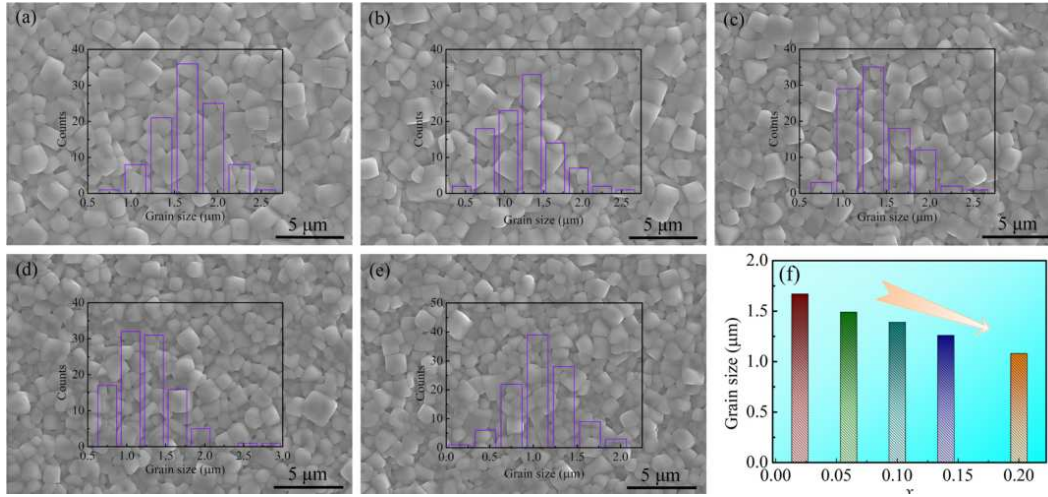


Figure 4. SEM micrographs of (NaBiBa)<sub>x</sub>(SrCa)<sub>(1-3x)/2</sub>TiO<sub>3</sub> ceramics (a-e) and average grain sizes and relative density (f) [37]



**Figure 5.** SEM images of morphologies and grain size distribution images of high-entropy  $(1-x)\text{BNKBCT}-x\text{BT}$  ceramics [38]

ually decreased, which facilitated the achievement of high electric breakdown field. Figure 4f shows the variation of relative density for different samples, as measured using the Archimedes drainage method. The relative density of all samples was above 95 %TD, indicating good sintering performance. The smaller grain size and higher density contributed to a higher electric breakdown field and improved energy storage characteristics.

Liu *et al.* [38] prepared perovskite high entropy  $(1-x)\text{Bi}_{0.5}\text{Na}_{0.5}\text{K}_{0.5}\text{Ba}_{0.5}\text{Ca}_{0.5}\text{TiO}_3-x\text{BaTiO}_3$  ceramics by solid state reaction method. The sintered ceramics had cubic grains with sharp grain edges (Fig. 5). Due to the edges and corners of the cubic grains, a number of micropores were formed. With an increase in  $\text{BaTiO}_3$  content, the lattice parameter gradually increases, which results in an increase in cell volume. A strong dispersion appears around the  $T_m$ , indicating that the prepared ceramics are relaxation ferroelectric ceramics. Due to the increase of lattice disorder and the relaxation and thermal evolution, the prepared ceramics exhibit a wide range of relaxation behaviours.

The high-entropy perovskite oxide ceramics,  $(\text{Bi}_{0.4}\text{Na}_{0.2}\text{K}_{0.2}\text{Ba}_{0.2})\text{TiO}_3-\text{Sr}(\text{Mg}_{1/3}\text{Nb}_{2/3})\text{O}_3$ , were prepared by Yan *et al.* [9]. The microstructure analysis reveals that the samples exhibit a relatively dense morphology with small grain sizes. Furthermore, the investigation demonstrates a significant correlation between the grain size of the ceramics and the content of constituent elements: as the content of the constituent elements increases, the grain size decreases. Conversely, an increase in the SMN content leads to an enlargement of the grain size.

#### 2.4. Niobate based high-entropy ceramics

Rai *et al.* [39] prepared  $\text{K}_{0.5}\text{Na}_{0.5}\text{NbO}_3-x\text{LiNbO}_3$  perovskite structured ferroelectric ceramics by the solid-state reaction method. The single phase was formed for pure  $\text{K}_{0.5}\text{Na}_{0.5}\text{NbO}_3$  while a small amount of second phase was present in KNN-LN ceramics. The electrical behaviour of the ceramics was studied by impedance spectroscopy and piezoelectric properties were also investigated.

Zhang *et al.* [40] fabricated niobate high-entropy  $(\text{La}_{0.2}\text{Li}_{0.2}\text{Ba}_{0.2}\text{Sr}_{0.2}\text{Ca}_{0.2})\text{Nb}_2\text{O}_6$  ceramics by solid-

state reaction. The prepared ceramics had tetragonal tungsten bronze structure after sintering at 1250–1350 °C, with densities up to 93 %TD and uniform grain distribution were obtained. Dielectric properties were also investigated and confirmed that entropy engineering is a credible strategy for tailoring properties of ceramic systems.

Lai *et al.* [41] prepared a series of high entropy rare earth niobates, including fluorite  $\text{Re}_3\text{NbO}_7$ , monoclinic  $\text{ReNbO}_4$  and  $\text{ReNbO}_4/\text{Re}_3\text{NbO}_7$  composites by solid phase reaction method and studied their thermal and mechanical properties. High entropy rare-earth niobate showed excellent phase stability after thermal exposure at 1300 °C for 100 h, indicating that entropy can stabilize high entropy rare-earth niobate. It is also proved that the configurational entropy has little effect on the critical temperature of the monoclinic-tetragonal phase transition.

### III. Properties of perovskite high-entropy oxides

#### 3.1. Dielectric properties

Although some progress has been made in the research of perovskite-type high-entropy oxide ceramics, the study of their dielectric properties is still lacking. For traditional perovskite ceramics like  $\text{SrTiO}_3$ , it is well known that changes in substitution types can lead to alterations in carrier concentration, such as oxygen vacancies, consequently influencing dielectric behaviour [42]. From the perspective of defect design, in order to maintain charge balance, oxygen vacancies or defect dipoles are typically introduced in materials to enhance dielectric performance.

Zhang *et al.* [43] synthesized high-entropy perovskite ceramics,  $\text{Li}_x(\text{BaSrCaMg})_{(1-x)/4}\text{TiO}_3$  ( $x = 0.1, 0.15, 0.2, 0.3$ ), using solid-state method, and systematically investigated the effects of Li content on the formation of ceramic phase, microstructure and the causes of dielectric relaxation. The results showed that all ceramics exhibited perovskite structure and the increase of Li content promoted grain growth and the formation of dense ceramics. The increase in Li content not only improved the dielectric constant but also resulted in high dielectric

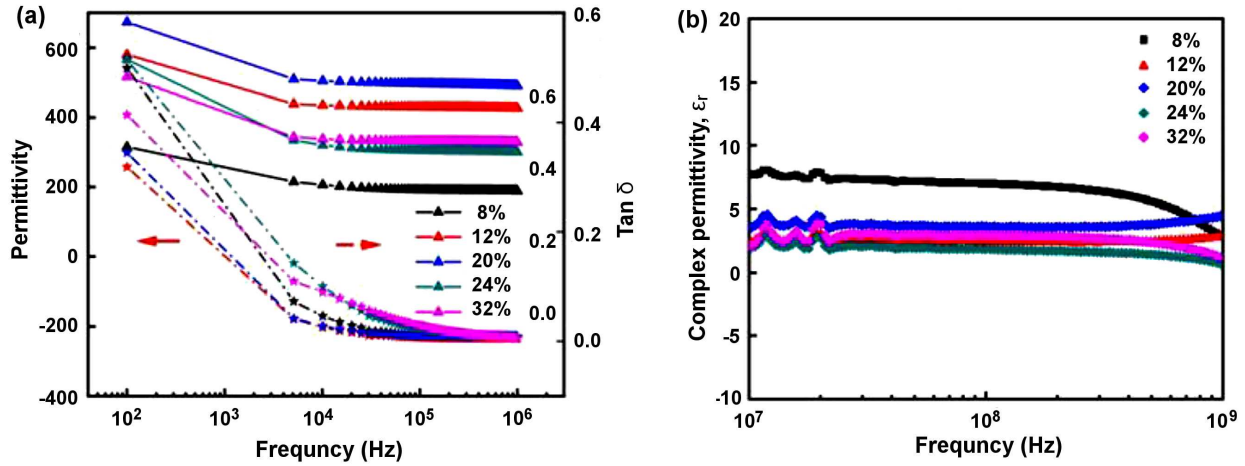


Figure 6. Dielectric spectra of  $(\text{Ce,K})_x[(\text{Bi,Na})\text{BaSrCa}]_{1-x}\text{TiO}_3$  ceramics at room temperature: a) low-frequency and b) high-frequency dielectric spectra [44]

loss. Low-temperature relaxation was caused by interfacial polarization, while high-temperature relaxation was attributed to the double ionized oxygen vacancies. At higher temperatures and lower frequencies, the rapid increase in dielectric constant was associated with the spatial charge of oxygen vacancies. The high-entropy effect can induce variations in the properties of perovskite oxide ceramics, with changes in dielectric performance being one of the core concerns for ceramic researchers.

Zhou *et al.* [44] fabricated a novel high entropy perovskite oxide  $(\text{Ce,K})_x[(\text{Bi,Na})\text{BaSrCa}]_{1-x}\text{TiO}_3$  ceramics by the traditional solid state reaction method. Microstructure analysis shows that the most uniform particles are obtained when  $x$  reaches 0.2. When the amounts of all elements are equal, the highest dielectric property can be detected, and the highest dielectric constant and the lowest dielectric loss can be measured, which are 535 and 0.04, respectively (Fig. 6). With the increase of frequency, the dielectric constant and dielectric loss both decrease to varying degrees, presenting a certain frequency dispersion and gradually stabilizing into a straight line until the frequency is greater than  $10^4$  Hz. Figure 6b shows the dielectric spectra in the high frequency range ( $10^7$ – $10^9$  Hz). It can be seen that the dielectric constant at higher frequencies is basically a straight line, showing a stable frequency state. When  $x = 0.08$ , the maximum dielectric constant is about 8.

Pu *et al.* [45] prepared single-phase and homogenous  $(\text{Na}_{0.2}\text{Bi}_{0.2}\text{Ba}_{0.2}\text{Sr}_{0.2}\text{Ca}_{0.2})\text{TiO}_3$  powder with high configurational entropy using the solid-state method. The study revealed that the perovskite structure exhibited a broad dielectric peak, which shifted towards higher temperatures with increasing frequency. This observation is consistent with the relaxation behaviour observed in other ferroelectric perovskite structures.

Zhou *et al.* [25] prepared a series of high-entropy  $\text{Ba}(\text{Zr}_{0.2}\text{Ti}_{0.2}\text{Sn}_{0.2}\text{Hf}_{0.2}\text{Me}_{0.2})\text{O}_3$  ( $\text{Me} = \text{Y}^{3+}, \text{Nb}^{5+}, \text{Ta}^{5+}, \text{V}^{5+}, \text{Mo}^{6+}, \text{W}^{6+}$ ) perovskite oxides using the solid-state reaction method. It can be clearly observed that these materials exhibit excellent stability in dielectric constant over a wide temperature range and have very low loss tangent ( $<0.002$ ) within the frequency range of 20 Hz to 2 MHz. Based on previous studies on how configura-

tional entropy affects thermal stability and electrochemical stability, it can be inferred that the stability of entropy also contributes to the stability of dielectric constant and loss tangent, as variations in these parameters can be attributed to the phase transitions and structural stability. Relatively low dielectric constants of the two ceramic samples can be attributed to the lower titanium content at the B-site and smaller grain sizes. Additionally, this result also indicates that the B-site sublattice has a significant impact on the dielectric and transport properties of perovskite oxides.

### 3.2. Energy storage characteristics

The energy storage characteristics of high-entropy perovskite oxide ceramics have been a recent focus of researchers, who aim to design and regulate the energy storage properties of these ceramics through structural manipulation. Lead-free ceramics are environmentally friendly; however, their energy storage performance is inferior to lead-containing ceramics. To address this, researchers have attempted to utilize the high-entropy strategy (Fig. 7) to design and regulate the structure of perovskite oxide ceramics for enhanced energy storage properties. Firstly, a large number of metal cations of different elements with different valence and different radii are introduced to enhance random fields and increase the chaos of the system, and high entropy is introduced to enhance  $P_{max}$  by taking advantage of the easy combination of  $2s$  and  $2p$  orbital hybridization of Pb and O. Moreover, the relaxation characteristics of ceramics are improved and the loop lines are refined by refining the grains and reducing the electric domain size. The breakdown electric field  $E_b$  of ceramics is increased by reducing grain size and the energy storage characteristics of ceramics are improved by increasing  $P_{max}$ , relaxation and hysteresis loops.

Qi *et al.* [47] fabricated high-entropy perovskite  $[(\text{Bi,Na})_{1/5}(\text{La,Li})_{1/5}(\text{Ce,K})_{1/5}\text{Ca}_{1/5}\text{Sr}_{1/5}]\text{TiO}_3$  ceramics and were the first who applied high-entropy perovskite in the field of lithium-ion batteries, where they can be used as catalytic carriers for hydrogen and oxygen evolution, particularly exhibiting great tunability in energy storage.

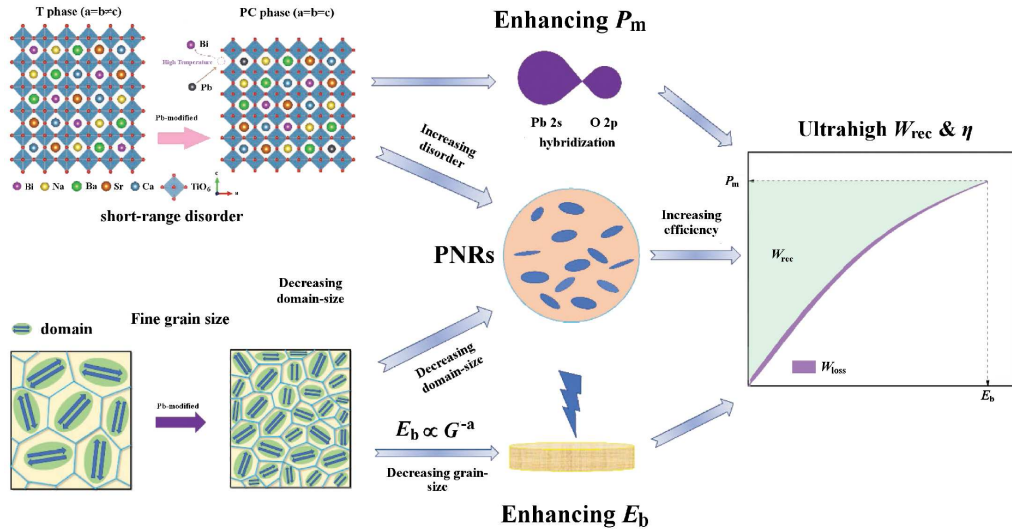


Figure 7. High-entropy ceramics energy storage density improvement strategy [46]

Chen *et al.* [48] added a significant amount of ions ( $\text{Li}^+$ ,  $\text{Ba}^{2+}$ ,  $\text{Bi}^{3+}$ ,  $\text{Sc}^{3+}$ ,  $\text{Hf}^{4+}$ ,  $\text{Zr}^{4+}$ ,  $\text{Ta}^{5+}$ ,  $\text{Sb}^{5+}$ ) with different ionic radii and valence states into the  $\text{K}_{0.2}\text{Na}_{0.8}\text{NbO}_3$  lattice to enhance the random field, stress field and electric field. This resulted in significant  $W_{rec}$  values, especially with  $\eta$  values as high as 90.8%, in lead-free relaxor ferroelectrics. Furthermore, these ceramics demonstrated good temperature stability (25–150 °C) and frequency stability (10–90 Hz). Additionally, excellent current density of 976.15 A/cm<sup>2</sup> and ultrahigh power density of 78.09 MW/cm<sup>3</sup> were achieved at 160 kV/cm.

Chen *et al.* [49] designed a series of lead-free perovskite-structured high-entropy ceramics by doping A and B-site ions. The composition of these ceramics was  $(\text{La}_{0.25}\text{Sr}_{0.25}\text{Ba}_{0.25}\text{Na}_{0.25})(\text{Ti}_{0.5}\text{Me}_{0.5})\text{O}_3$  (Me = Sn, Zr, Hf). High-entropy ceramics exhibited typical relaxor characteristics. The ceramics with Sn addition achieved a discharge energy density ( $W_d$ ) of 0.31 J/cm<sup>3</sup> and energy storage efficiency ( $\eta$ ) of 90.88%.

Although lead-containing ceramics have certain environmental pollution concerns, their excellent energy storage properties have led to significant research efforts in exploring lead-containing high-entropy ceramic structures, yielding promising results. Guo *et al.* [50] achieved high-entropy effects by Pb-doping into  $\text{Bi}_{0.25}\text{Na}_{0.25}\text{Sr}_{0.5}\text{TiO}_3$  relaxor ferroelectric ceramics. The high-entropy ceramics demonstrated a  $W_{rec}$  of 5.2 J/cm<sup>3</sup> and  $\eta$  of 82%, along with good charge-discharge performance, including a discharge speed of 24 ns and power density of 296 MW/cm<sup>3</sup>. These remarkable comprehensive results suggest the potential application prospects of these ceramics.

Not only Pb elements, but the intervention of other metal elements can also enhance the energy storage characteristics of perovskite oxide high-entropy ceramics to some extent. Kumar *et al.* [51] investigated the energy storage performance of manganese-doped  $(\text{Pb}_{0.93}\text{La}_{0.07})(\text{Zr}_{0.82}\text{Ti}_{0.18})\text{O}_3$  antiferroelectric ceramics. The study found that 0.2% Mn-doped PLZT ceramics exhibited the highest energy storage density of 460 J/cm<sup>3</sup> and the best energy storage efficiency of 63%.

He *et al.* [52] fabricated lead-free ceramics by adding  $\text{Sr}_{1/2}\text{La}_{1/3}(\text{Ti}_{0.7}\text{Zr}_{0.3})\text{O}_3$  into the  $(\text{Bi}_{0.5}\text{Na}_{0.5})_{0.7}\text{Sr}_{0.3}\text{TiO}_3$  matrix. Under the low electric field condition of 170 kV/cm, the ceramics with 10%  $\text{Sr}_{1/2}\text{La}_{1/3}(\text{Ti}_{0.7}\text{Zr}_{0.3})\text{O}_3$  demonstrated good energy storage performance with a  $W_{rec}$  of 2.06 J/cm<sup>3</sup> and  $\eta$  of 90.6%.

Li *et al.* [53] introduced a perovskite high-entropy ceramic compound,  $\text{Bi}(\text{Li}_{0.2}\text{Y}_{0.2}\text{Mg}_{0.2}\text{Ti}_{0.2}\text{Ta}_{0.2})\text{O}_3$ , into the  $0.9\text{Ba}(\text{Ti}_{0.97}\text{Ca}_{0.03})\text{O}_3$ -0.1 $\text{Bi}_{0.55}\text{Na}_{0.45}\text{TiO}_3$  matrix. At an electric field of 240 kV/cm, the ceramics achieved both a high energy storage density of 4.89 J/cm<sup>3</sup> and an energy storage efficiency of 91.2%. Liu *et al.* [54] prepared high-entropy  $(\text{Bi}_{0.2}\text{Na}_{0.2}\text{K}_{0.2}\text{Ba}_{0.2}\text{Ca}_{0.2})\text{TiO}_3$  ceramics through spark plasma sintering. Uniform distribution of elements and a single-phase perovskite ceramics with lattice distortion were achieved in the high-entropy ceramics, which exhibited relaxor behaviour. Under an electric field of 129 kV/cm, the discharge energy storage density and energy storage efficiency of the high-entropy ceramics were 0.684 J/cm<sup>3</sup> and 87.5%, respectively. Additionally, in this high-entropy ceramics, excessive  $\text{Na}^+$  and  $\text{K}^+$  formed electrically active defects due to the charge compensation, thereby improving the breakdown field strength. The study demonstrates that the high-entropy strategy is an effective mean of adjusting the properties of BNT-based ceramics.

Ma *et al.* [55] fabricated lead-free  $(1-x)\text{BaTiO}_3$ - $x\text{Bi}(\text{Y}_{1/3}\text{Ti}_{1/2})\text{O}_3$  ceramics (referred to as  $(1-x)\text{BT}$ - $x\text{BYT}$ ) using the solid-state method and investigated the effect of component compositions on the ceramics' properties. The study revealed that with the increasing BYT content, higher polarization saturation ( $P_{max}$ ), lower remanent polarization ( $P_r$ ), and narrower  $P$ - $E$  hysteresis loops could be observed. When  $x = 0.15$ , the energy storage density ( $W_{rec}$ ) was 1.02 J/cm<sup>3</sup> with an efficiency ( $\eta$ ) of 78%. On the other hand, when  $x = 0.2$ , the energy storage density ( $W_{rec}$ ) decreased to 0.77 J/cm<sup>3</sup> with an improved efficiency ( $\eta$ ) of 90%. In addition, Yan *et al.* [9] employed multi-ion doping in the same  $\text{BaTiO}_3$  system and designed and fabricated high-entropy perovskite oxides

in the  $(\text{Bi}_{0.4}\text{Na}_{0.2}\text{K}_{0.2}\text{Ba}_{0.2})\text{TiO}_3\text{-Sr}(\text{Mg}_{1/3}\text{Nb}_{2/3})\text{O}_3$  system for dielectric energy storage. Under a voltage of 310 kV/cm, the ceramics exhibited a recoverable energy storage density of 3.37 J/cm<sup>3</sup> and an energy storage efficiency of 80%, making it the highest energy density achieved at low electric fields.

Similar to the high-entropy strontium niobate system, the silver niobate high-entropy system also deserves attention. Zheng *et al.* [56] prepared lead-free ceramics of  $(1-x)[(\text{Bi}_{0.5}\text{Na}_{0.5})_{0.94}\text{Ba}_{0.06}\text{TiO}_3]_x\text{AgNbO}_3$  (abbreviated as BNTBT-100xAN) by solid-state method. Experimental results revealed that the addition of AgNbO<sub>3</sub> reduced the residual polarization of BNTBT-5AN ceramics and improved the dielectric breakdown strength. Under an electric field of 105 kV/cm, the effective energy storage density of BNTBT-5AN ceramics was 1.27 J/cm<sup>3</sup> with a conversion efficiency of 77.5%.

Zahid *et al.* [57] employed sol-gel method to fabricate  $(\text{BaTi}_{0.89}\text{Sn}_{0.11}\text{O}_3)$  ceramics. The ceramics exhibited a high dielectric constant of 15460 and low dielectric loss over a wide temperature range. At an external electric field change of 35 kV/cm, near room temperature, the energy storage density of the ceramics was 122 mJ/cm<sup>3</sup> with an efficiency of 79%. Nandan *et al.* [58] synthesized lead-free  $\text{Ba}_{0.85}\text{Ca}_{0.15}\text{Hf}_{0.10}\text{Ti}_{0.90}\text{O}_3$  ferroelectric ceramics using sol-gel method. Under low electric field of 20 kV/cm at room temperature, the total energy density, recoverable energy density, and energy storage efficiency of the ceramics were improved to 84.43 mJ/cm<sup>3</sup>, 64.38 mJ/cm<sup>3</sup> and 76.25%, respectively. The highest energy storage efficiency was achieved at 80 °C, reaching 85.03%.

Dahri *et al.* [59] prepared lead-free  $\text{Ba}_{0.90}\text{Ca}_{0.10}\text{Zr}_{0.15}\text{Ti}_{0.85}\text{O}_3$  ferroelectric ceramics using the conventional solid-state method near the phase coexistence region. In the temperature range from 27 to 60 °C and 27 to 100 °C, the thermal stability of  $W_{rec}$  was 3.64% and 16.08% at  $E_1 = 11$  kV/cm and  $E_2 = 26.16$  kV/cm, respectively. At  $E_2 = 26.16$  kV/cm, the maximum  $W_{rec}$  value obtained at room temperature was 140.7 mJ/cm<sup>3</sup> with an energy efficiency of 42.5%.

Khardazi *et al.* [60] prepared perovskite-type  $\text{Ba}_{0.9}\text{Sr}_{0.1}\text{Ti}_{0.9}\text{Sn}_{0.1}\text{O}_3$  ceramics using sol-gel method. The  $P$ - $E$  hysteresis loops of the ceramics were recorded at different temperatures, and the ferroelectric and energy storage properties of the ceramics were investigated. At room temperature, under a moderate electric field of 20 kV/cm, the recoverable energy density and energy storage efficiency of the ceramics were improved to 58.08 mJ/cm<sup>3</sup> and 84.36%, respectively.

Qi *et al.* [61] designed a high configurational entropy (HCE) material,  $\text{BaTiO}_3\text{-BiFeO}_3\text{-CaTiO}_3$ , with rational microstructure engineering, exhibiting an ultra-high energy density of 7.2 J/cm<sup>3</sup>. The HCE design improved the solubility of CaTiO<sub>3</sub> in the matrix, increasing the resistivity and polarization. Meanwhile, due to the strong scattering of electron carriers and obstacles to the breakdown path, the nanosegregation around the grains significantly improved the breakdown strength. The energy density of multilayer ceramic capacitors constructed using this dielectric reached 16.6 J/cm<sup>3</sup>, with an energy storage efficiency of up to 83%.

Wang *et al.* [62] fabricated

$\text{Pb}_{0.97}\text{La}_{0.02}(\text{Zr}_{0.46-x}\text{Sn}_{0.54}\text{Ti}_x)\text{O}_3$  antiferroelectric thick film materials using tape casting method. At ambient temperature, the maximum energy density of the thick film ceramic was 5.2 J/cm<sup>3</sup> under a field of 600 kV/cm, with an efficiency of 78.2%.

### 3.3. Other properties

High-entropy perovskite ceramics not only exhibit excellent dielectric properties and high energy storage density, but also possess significant advantages in other structural properties. Kumar *et al.* [63] investigated the electrocaloric effect (ECE) of  $(1-x)\text{K}_{0.5}\text{Na}_{0.5}\text{NbO}_3\text{-xLiNbO}_3$  (KNN- $x$ LiN) nanoceramics in the range of  $0.01 \leq x \leq 0.05$  using the Maxwell indirect measurement method. At  $x = 0.01, 0.03$  and  $0.05$  the maximum values of ECE for the cathode and anode were  $-0.40$  and  $0.24$  K,  $-0.23$  and  $0.18$  K, and  $-0.13$  and  $0.29$  K, respectively. For  $x = 0.01, 0.03$  and  $0.05$ , at an electric field intensity of 45 kV/cm, the energy storage efficiencies were 30%, 50% and 51%, respectively, and the maximum recoverable energy densities were 0.12, 0.13 and 0.128 J/cm<sup>3</sup>, respectively. In terms of structural performance, impressive results can also be achieved using a pure phase perovskite high-entropy ceramic system.

Zhou *et al.* [25] synthesized a series of high-entropy  $\text{Ba}(\text{Zr}_{0.2}\text{Ti}_{0.2}\text{Sn}_{0.2}\text{Hf}_{0.2}\text{Me}_{0.2})\text{O}_3$  perovskite oxides using the solid-state reaction method. Through dielectric property testing, the high-entropy ceramics exhibited good temperature stability within the range of 25 to 200 °C, with a dielectric loss below 0.002 in the frequency range of 20 Hz to 2 MHz, high resistance, and moderate breakdown strengths (290 kV/cm, 370 kV/cm). This experiment strongly confirms that the control of configurational entropy may provide a feasible perspective for establishing highly tunable perovskite structures and exploring novel dielectric materials.

## IV. Conclusions and outlook

Compared to traditional ceramic materials, high-entropy ceramics have gained extensive research interest due to their superior energy storage properties, attributed to thermodynamic high-entropy effects, kinetic hysteresis diffusion effects, structural lattice distortion effects and performance “cocktail” mixing effects. In recent years, significant progress has been made in the design, controllable preparation and performance of high-entropy ceramics by researchers worldwide. However, there are still some challenges that need to be addressed by researchers all over the world.

1. The research on high-entropy ceramics has mainly focused on five-component equimolar materials. More researchers are needed to design new component high-entropy ceramics, which is one of the future research directions in the field. Moreover, most high-entropy ceramic systems developed so far are oxides, nitrides, carbides, borides, etc. Therefore, the development of new ceramic systems remains a key focus in high-entropy ceramics research.
2. The preparation process of high-entropy ceramics is crucial. Due to the involvement of multiple elements, there is a higher likelihood of element loss during the

preparation process. Therefore, continuous improvement of the preparation techniques is necessary to minimize or avoid element loss.

3. Although high-entropy ceramics generally exhibit superior properties compared to ordinary ceramics, there are still some aspects of their performance that require further investigation. Extensive comparative experiments are needed to fully understand the strengths and limitations of high-entropy ceramics. While much research has been conducted on single-phase high-entropy ceramics, the development of composite high-entropy ceramics has also shown excellent performance, making it worthy of further exploration.
4. With the advancement of technology, an increasing number of materials researchers are inclined to combine experimental approaches with computer software. The study of new high-entropy ceramic systems also relies on the integration of computer software. While software development for high-entropy alloys has matured, there is still a need for more advanced software development specifically tailored for high-entropy ceramics.

In summary, the field of high-entropy ceramics presents exciting prospects for future research and development. By addressing the aforementioned challenges, researchers can further unlock the potential of high-entropy ceramics and contribute to their application in various fields. The high entropy ceramics of many systems are screened through calculation and high throughput experimental design. The properties of known high entropy ceramics are explored, the application range of high entropy ceramics is enriched, and the root cause of their extraordinary properties is explained by simulation calculations. High-entropy ceramics are developing from the current solid solution of five or more components in equal proportion to a wider number of components, such as three, four or six components and more, and the proportion of each element is also developing from equal proportion to nearly equal proportion, so as to achieve the control of internal defects of high-entropy ceramics, and further explore the influence of defects on the performance of high-entropy ceramics. High-entropy ceramics are combined with other materials to further expand their application fields.

## References

1. M. Zhang, X. Zhang, S. Das, Z. M. Wang, X. Qi, Q. Du, "High remanent polarization and temperature-insensitive ferroelectric remanent polarization in BiFeO<sub>3</sub>-based lead-free perovskite", *J. Mater. Chem. C*, **7** [34] (2019) 10551–10560.
2. G. Dong, S. Ma, J. Du, J. Cui, "Dielectric properties and energy storage density in ZnO-doped Ba<sub>0.3</sub>Sr<sub>0.7</sub>TiO<sub>3</sub> ceramics", *Ceram. Int.*, **35** [5] (2009) 2069–2075.
3. K.D. Kreuer, "Proton-conducting oxides", *Annu. Rev. Mater. Res.*, **33** [1] (2003) 333–359.
4. M.S. Wrighton, D.L. Morse, A.B. Ellis, D.S. Ginley, H.B. Abrahamson, "Photoassisted electrolysis of water by ultraviolet irradiation of an antimony doped stannic oxide electrode", *J. Am. Chem. Soc.*, **9**, [1] (1976) 44–48.
5. L. Ji, M.D. McDaniel, S. Wang, A.B. Posadas, X. Li, H. Huang, J.C. Lee, A.A. Demkov, A.J. Bard, J.G. Ekerdt, E.T. Yu, "A silicon-based photocathode for water reduction with an epitaxial SrTiO<sub>3</sub> protection layer and a nanostructured catalyst", *Nat. Nanotech.*, **10** [1] (2015) 84–90.
6. S. Zhou, Y. Pu, X. Zhang, Y. Shi, Z. Gao, Y. Feng, G. Shen, X. Wang, D. Wang, "High energy density, temperature stable lead-free ceramics by introducing High-entropy perovskite oxide", *Chem. Eng. J.*, **427** (2022) 131684.
7. A.S. Bhalla, R. Guo, R. Roy, "The perovskite structure - A review of its role in ceramic science and technology", *Mater. Res. Innovat.*, **4** [1] (2000) 3–26.
8. C.-W. Ahn, D. Maurya, C.-S. Park, S. Nahm, S. Priya, "A generalized rule for large piezoelectric response in perovskite oxide ceramics and its application for design of lead-free compositions", *J. Appl. Phys.*, **105** [11] (2009) 114108.
9. B. Yan, K. Chen, L. An, "Design and preparation of lead-free (Bi<sub>0.4</sub>Na<sub>0.2</sub>K<sub>0.2</sub>Ba<sub>0.2</sub>)TiO<sub>3</sub>-Sr(Mg<sub>1/3</sub>Nb<sub>2/3</sub>)O<sub>3</sub> high-entropy relaxor ceramics for dielectric energy storage", *Chem. Eng. J.*, **453** (2023) 139921.
10. B. Gludovatz, A. Hohenwarter, D. Catoor, E.H. Chang, E.P. George, R.O. Ritchie, "A fracture-resistant high-entropy alloy for cryogenic applications", *Science*, **345** [6201] (2014) 1153–1158.
11. Y. Deng, C.C. Tasan, K.G. Pradeep, H. Springer, A. Kostka, D. Raabe, "Design of a twinning-induced plasticity high-entropy alloy", *Acta Mater.*, **94** (2015) 124–133.
12. Z. Zhang, M.M. Mao, J. Wang, B. Gludovatz, Z. Zhang, S.X. Mao, E.P. George, Q. Yu, R.O. Ritchie, "Nanoscale origins of the damage tolerance of the high-entropy alloy CrMnFeCoNi", *Nat. Commun.*, **6** [1] (2015) 10143.
13. J.-W. Yeh, S.-K. Chen, S.-J. Lin, J.-Y. Gan, T.-S. Chin, T.-T. Shun, C.-H. Tsau, S.-Y. Chang, "Nanostructured high-entropy alloys with multiple principal elements: Novel alloy design concepts and outcomes", *Adv. Eng. Mater.*, **6** [5] (2004) 299–303.
14. R.-Z. Zhang, M.J. Reece, "Review of high entropy ceramics: design, synthesis, structure and properties", *J. Mater. Chem. A*, **7** (2019) 22148–22162.
15. S. Akrami, P. Edalati, M. Fuji, K. Edalati, "High-entropy ceramics: Review of principles, production and applications", *Mater. Sci. Eng. R*, **146** (2021) 100644.
16. T.C. Dube, J. Zhang, "Underpinning the relationship between synthesis and properties of high entropy ceramics: A comprehensive review on borides, carbides and oxides", *J. Eur. Ceram. Soc.*, **44** [3] (2024) 1335–1350.
17. M.W. Glasscott, "Classifying and benchmarking high-entropy alloys and associated materials for electrocatalysis: A brief review of best practices", *Curr. Opinion Electrochem.*, **34** (2022) 100976.
18. C.M. Rost, E. Sachet, T. Borman, A. Moballeggh, E.C. Dickey, D. Hou, J.L. Jones, S. Curtarolo, J.-P. Maria, "Entropy-stabilized oxides," *Nat. Commun.*, **6** [1] (2015) 8485.
19. N. Dragojević, D. Bérardan, "Order emerging from disorder: Entropy stabilization provides a new direction for developing functional materials", *Science*, **366** [6465] (2019) 573–574.
20. M. Biesuz, L. Spiridigliozzi, G. Dell'Agli, M. Bortolotti, V.M. Sglavo, "Synthesis and sintering of (Mg,Co,Ni,Cu,Zn)O entropy-stabilized oxides obtained by wet chemical methods", *J. Mater. Sci.*, **53** [11] (2018)

- 8074–8085.
21. A. Kimbauer, C. Spadt, C.M. Koller, S. Koložsvári, P.H. Mayrhofer, “High-entropy oxide thin films based on Al-Cr-Nb-Ta-Ti”, *Vacuum*, **168** (2019) 108850.
  22. A.J. Wright, Q. Wang, C. Huang, A. Nieto, R. Chen, J. Luo, “From high-entropy ceramics to compositionally-complex ceramics: A case study of fluorite oxides”, *J. Eur. Ceram. Soc.*, **40** [5] (2020) 2120–2129.
  23. J. Gild, M. Samiee, J.L. Braun, T. Harrington, H. Vega, P.E. Hopkins, K. Vecchio, J. Luo, “High-entropy fluorite oxides”, *J. Eur. Ceram. Soc.*, **38** [10] (2018) 3578–3584.
  24. D. Bérardan, S. Franger, D. Dragoë, A.K. Meena, N. Dragoë, “Colossal dielectric constant in high-entropy oxides”, *Phys. Status Solidi RRL*, **10** [4] (2016) 328–333.
  25. S. Zhou, Y. Pu, Q. Zhang, R. Shi, X. Guo, W. Wang, J. Ji, T. Wei, T. Ouyang, “Microstructure and dielectric properties of high-entropy Ba(Zr<sub>0.2</sub>Ti<sub>0.2</sub>Sn<sub>0.2</sub>Hf<sub>0.2</sub>Me<sub>0.2</sub>)O<sub>3</sub> perovskite oxides”, *Ceram. Int.*, **46** [6] (2020) 7430–7437.
  26. P. Edalati, Q. Wang, H. Razavi-Khosroshahi, M. Fujii, T. Ishihara, K. Edalati, “Photocatalytic hydrogen evolution on a high-entropy oxide”, *J. Mater. Chem. A*, **8** [7] (2020) 3814–3821.
  27. T. Parida, A. Karati, K. Guruvadyathri, B.S. Murty, G. Markandeyulu, “Novel rare-earth and transition metal-based entropy stabilized oxides with spinel structure”, *Scripta Mater.*, **178**, (2020) 513–517.
  28. Y. Zheng, Y. Yi, M. Fan, H. Liu, X. Li, R. Zhang, M. Li, Z.-A. Qiao, “A high-entropy metal oxide as chemical anchor of polysulfide for lithium-sulfur batteries”, *Energy Storage Mater.*, **23** (2019) 678–683.
  29. Y. Kong, S. Hu, C. Cai, Z. Wang, S. Zhang, “Processing and electrical conductivity property of lithium-doped high-entropy pyrochlore and perovskite ceramics”, *Process. Appl. Ceram.*, **17** [3] (2023) 264–270.
  30. S. Jiang, T. Hu, J. Gild, N. Zhou, J. Nie, M. Qin, T. Harrington, K. Vecchio, J. Luo, “A new class of high-entropy perovskite oxides”, *Scripta Mater.*, **142** (2018) 116–120.
  31. M. Biesuz, S. Fu, J. Dong, A. Jiang, D. Ke, Q. Xu, D. Zhu, M. Bortolotti, M.J. Reece, C. Hu, S. Grasso, “High-entropy Sr((Zr<sub>0.94</sub>Y<sub>0.06</sub>)<sub>0.2</sub>Sn<sub>0.2</sub>Ti<sub>0.2</sub>Hf<sub>0.2</sub>Mn<sub>0.2</sub>)O<sub>3-x</sub> perovskite synthesis by reactive spark plasma sintering”, *J. Asian Ceram. Soc.*, **7** [2] (2019) 127–132.
  32. P. Zhang, Z. Lou, M. Qin, J. Xu, J. Zhu, Z. Shi, Q. Chen, M.J. Reece, H. Yan, F. Gao, “High-entropy (Ca<sub>0.2</sub>Sr<sub>0.2</sub>Ba<sub>0.2</sub>La<sub>0.2</sub>Pb<sub>0.2</sub>)TiO<sub>3</sub> perovskite ceramics with A-site short-range disorder for thermoelectric applications”, *J. Mater. Sci. Technol.*, **97** (2022) 182–189.
  33. A. Sarkar, R. Djenadic, D. Wang, C. Hein, R. Kautenburger, O. Clemens, H. Hahn, “Rare earth and transition metal based entropy stabilised perovskite type oxides”, *J. Eur. Ceram. Soc.*, **38** [5] (2018) 2318–2327.
  34. S. Schweidler, Y. Tang, L. Lin, G. Karkera, A. Alsawaf, L. Bernadet, B. Breitung, H. Hahn, M. Fichtner, A. Tarancon, M. Botros, “Synthesis of perovskite-type high-entropy oxides as potential candidates for oxygen evolution”, *Front. Energy Res.*, **10** (2022) 983979.
  35. C. Zhou, X. Zhang, S. Li, J. Yan, X. Qi, “Dielectric and energy storage properties of (La,Li)<sub>x</sub>[(Bi,Na)BaSrCa]<sub>1-x</sub>TiO<sub>3</sub> high-entropy perovskite ceramics”, *Ceram. Int.*, **48** [17] (2022) 24268–24274.
  36. W. Sun, F. Zhang, X. Zhang, T. Shi, J. Li, Y. Bai, C. Wang, Z. Wang, “Enhanced electrical properties of (Bi<sub>0.2</sub>Na<sub>0.2</sub>Ba<sub>0.2</sub>Ca<sub>0.2</sub>Sr<sub>0.2</sub>)TiO<sub>3</sub> high-entropy ceramics prepared by hydrothermal method”, *Ceram. Int.*, **48** [13] (2022) 19492–19500.
  37. Y. Ning, Y. Pu, Q. Zhang, S. Zhou, C. Wu, L. Zhang, Y. Shi, Z. Sun, “Achieving high energy storage properties in perovskite oxide via high-entropy design”, *Ceram. Int.*, **49** [8] (2023) 12214–12223.
  38. J. Liu, C. Ma, X. Zhao, K. Ren, R. Zhang, F. Shang, H. Du, Y. Wang, “Structure, dielectric, and relaxor properties of BaTO<sub>3</sub>-modified high-entropy (Bi<sub>0.2</sub>Na<sub>0.2</sub>K<sub>0.2</sub>Ba<sub>0.2</sub>Ca<sub>0.2</sub>)TiO<sub>3</sub> ceramics for energy storage applications”, *J. Alloys Compd.*, **947** (2023) 169626.
  39. R. Rai, I. Coondoo, R. Rani, I. Bdikin, S. Sharma, A.L. Kholkin, “Impedance spectroscopy and piezoresponse force microscopy analysis of lead-free (1-x)K<sub>0.5</sub>Na<sub>0.5</sub>NbO<sub>3</sub>-xLiNbO<sub>3</sub> ceramics”, *Curr. Appl. Phys.*, **13** [2] (2013) 430–440.
  40. X. Zhang, J. Li, B. Ni, R. Yang, H. Xie, S. Yang, X. Qi, “Dielectric properties of novel high-entropy (La<sub>0.2</sub>Li<sub>0.2</sub>Ba<sub>0.2</sub>Sr<sub>0.2</sub>Ca<sub>0.2</sub>)Nb<sub>2</sub>O<sub>6-δ</sub> tungsten bronze ceramics”, *J. Mater. Sci.*, **57** [33] (2022) 15901–15912.
  41. L. Lai, M. Gan, J. Wang, L. Chen, X. Liang, J. Feng, X. Chong, “New class of high-entropy rare-earth niobates with high thermal expansion and oxygen insulation”, *J. Am. Ceram. Soc.*, **106** [7] (2023) 4343–4357.
  42. W. Pan, M. Cao, H. Hao, Z. Yao, Z. Yu, H. Liu, “Defect engineering toward the structures and dielectric behaviors of (Nb, Zn) co-doped SrTiO<sub>3</sub> ceramics”, *J. Eur. Ceram. Soc.*, **40** [1] (2020) 49–55.
  43. J. Zhang, H. Liu, Y. Gu, J. Zhang, X. Zhang, X. Qi, “Oxygen-vacancy-related dielectric relaxations and electrical properties in [Li<sub>x</sub>(BaSrCaMg)<sub>(1-x)/4</sub>]TiO<sub>3</sub> high-entropy perovskite ceramics”, *J. Mater. Sci. Mater. Electron.*, **33** [13] (2022) 9918–9929.
  44. J. Zhou, P. Li, X. Zhang, J. Yan, X. Qi, “Effect of configurational entropy on dielectric properties of high-entropy perovskite oxides (Ce<sub>0.5</sub>K<sub>0.5</sub>)<sub>x</sub>[(Bi<sub>0.5</sub>Na<sub>0.5</sub>)<sub>0.25</sub>Ba<sub>0.25</sub>Sr<sub>0.25</sub>Ca<sub>0.25</sub>]<sub>1-x</sub>TiO<sub>3</sub>”, *J. Mater. Sci. Mater. Electron.*, **33** [26] (2022) 20721–20730.
  45. Y. Pu, Q. Zhang, R. Li, M. Chen, X. Du, S. Zhou, “Dielectric properties and electrocaloric effect of high-entropy (Na<sub>0.2</sub>Bi<sub>0.2</sub>Ba<sub>0.2</sub>Sr<sub>0.2</sub>Ca<sub>0.2</sub>)TiO<sub>3</sub> ceramic”, *Appl. Phys. Lett.*, **115** [22] (2019) 223901.
  46. J. Guo, W. Xiao, X. Zhang, J. Zhang, J. Wang, G. Zhang, S.-T. Zhang, “Achieving excellent energy storage in fine-grained high-entropy relaxor ferroelectric ceramics”, *Adv. Electron. Mater.*, **8** (2022) 2200503.
  47. J. Yan, D. Wang, X. Zhang, J. Li, Q. Du, X. Liu, J. Zhang, X. Qi, “A high-entropy perovskite titanate lithium-ion battery anode”, *J. Mater. Sci.*, **55** [16] (2020) 6942–6951.
  48. L. Chen, S. Deng, H. Liu, J. Wu, H. Qi, J. Chen, “Giant energy-storage density with ultrahigh efficiency in lead-free relaxors via high-entropy design”, *Nat. Commun.*, **13** [1] (2022) 3089.
  49. Y. Chen, R. Li, Y. Zhang, Y. Long, N. Liu, H. Xia, X. Luo, B. Meng, “Preparation and dielectric properties of lead-free perovskite-structured high-entropy ceramics of (La<sub>0.25</sub>Sr<sub>0.25</sub>Ba<sub>0.25</sub>Na<sub>0.25</sub>)(Ti<sub>0.5</sub>Me<sub>0.5</sub>)O<sub>3-δ</sub> (Me = Sn, Zr, Hf) via doping at both A and B sites”, *Ceram. Int.*, **49** [1] (2023) 1038–1047.
  50. J. Guo, X. Fan, J. Zhang, S.-T. Zhang, B. Yang, “Giant comprehensive energy storage performance in Pb-doped

- Bi<sub>0.25</sub>Na<sub>0.25</sub>Sr<sub>0.5</sub>TiO<sub>3</sub> ceramics via multiscale regulation of grain size and relaxation behavior”, *J. Eur. Ceram. Soc.*, **43** [4] (2023) 1523–1530.
51. A. Kumar, G. Lee, Y.G. Chae, A. Thakre, H.S. Choi, G.H. Nam, J. Ryu, “Induced slim ferroelectric hysteresis loops and enhanced energy-storage properties of Mn-doped (Pb<sub>0.93</sub>La<sub>0.07</sub>)(Zr<sub>0.82</sub>Ti<sub>0.18</sub>)O<sub>3</sub> anti-ferroelectric thick films by aerosol deposition”, *Ceram. Int.*, **47** [22] (2021) 31590–31596.
  52. X. He, Y. Wang, H. Wang, Y. Chen, X. Wang, C. Xu, Q. Zheng, Y. Chen, W. He, D. Lin., “Synchronously enhancing energy storage density, efficiency and power density under low electric field in lead-free ferroelectric (1-x)(Bi<sub>0.5</sub>Na<sub>0.5</sub>)<sub>0.7</sub>Sr<sub>0.3</sub>TiO<sub>3</sub>-xSr<sub>1/2</sub>La<sub>1/3</sub>(Ti<sub>0.7</sub>Zr<sub>0.3</sub>)O<sub>3</sub> ceramics”, *J. Alloys Compd.*, **922** (2022) 166049.
  53. Z. Li, Z. Chen, J. Xu, “Enhanced energy storage performance of BaTi<sub>0.97</sub>Ca<sub>0.03</sub>O<sub>2.97</sub>-based ceramics by doping high-entropy perovskite oxide”, *J. Alloys Compd.*, **922** (2022) 166179.
  54. J. Liu, K. Ren, C. Ma, H. Du, Y. Wang, “Dielectric and energy storage properties of flash-sintered high-entropy (Bi<sub>0.2</sub>Na<sub>0.2</sub>K<sub>0.2</sub>Ba<sub>0.2</sub>Ca<sub>0.2</sub>)TiO<sub>3</sub> ceramic”, *Ceram. Int.*, **46** [12] (2020) 20576–20581.
  55. C. Ma, H. Du, J. Liu, L. Kang, X. Du, X. Xi, H. Ran, “High-temperature stability of dielectric and energy-storage properties of weakly-coupled relaxor (1-x)BaTiO<sub>3</sub>-xBi(Y<sub>1/3</sub>Ti<sub>1/2</sub>)O<sub>3</sub> ceramics”, *Ceram. Int.*, **47** [17] (2021) 25029–25036.
  56. S. Zheng, Q. Li, Y. Chen, A. K. Yadav, W. Wang, H. Fan, “Enhanced energy storage density with excellent temperature-stable dielectric properties of (1-x)[(Bi<sub>0.5</sub>Na<sub>0.5</sub>)<sub>0.94</sub>Ba<sub>0.06</sub>TiO<sub>3</sub>]-xAgNbO<sub>3</sub> lead-free ceramics”, *J. Alloys Compd.*, **911** (2022) 165019.
  57. M. Zahid, Y. Hadouch, M. Amjoud, D. Mezzane, M. Gouné, K. Houmada, A. Alimoussa, A.G. Razumnaya, B. Rožič, Z. Kutnjak, “Enhanced near-ambient temperature energy storage and electrocaloric effect in the lead-free BaTi<sub>0.89</sub>Sn<sub>0.11</sub>O<sub>3</sub> ceramic synthesized by sol-gel method”, *J. Mater. Sci. Mater. Electron.*, **33** [16] (2022) 12900–12911.
  58. R. Nandan, S. Kumar, N.S. Negi, “High energy storage efficiency and electrocaloric effect in Pb-free Ba<sub>0.85</sub>Ca<sub>0.15</sub>Hf<sub>0.10</sub>Ti<sub>0.90</sub>O<sub>3</sub> ceramics for sustainable green energy applications”, *ECS Trans.*, **107** [1] (2022) 1996.
  59. A. Dahri, Y. Gagou, N. Abdelmoula, H. Khemakhem, M. El Marssi, “The structural, dielectric, electrocaloric, and energy storage properties of lead-free Ba<sub>0.90</sub>Ca<sub>0.10</sub>Zr<sub>0.15</sub>Ti<sub>0.85</sub>O<sub>3</sub>”, *Ceram. Int.*, **48** [3] (2022) 3157–3171.
  60. S. Khardazi, H. Zaitouni, S. Belkhadir, D. Mezzane, M. Amjoud, Y. Gagou, B. Asbani, I. Lukyanchuk, S. Terenchuk, “Improvement of the electrocaloric effect and energy storage performances in Pb-free ferroelectric Ba<sub>0.9</sub>Sr<sub>0.1</sub>Ti<sub>0.9</sub>Sn<sub>0.1</sub>O<sub>3</sub> ceramic near room temperature”, *J. Solid State Chem.*, **311** (2022) 123112.
  61. J. Qi, M. Zhang, Y. Chen, Z. Luo, P. Zhao, H. Su, J. Wang, H. Wang, L. Yang, H. Pan, S. Lan, Z.-H. Shen, D. Yi, Y.-H. Lin, “High-entropy assisted BaTiO<sub>3</sub>-based ceramic capacitors for energy storage”, *Cell Reports Phys. Sci.*, **3** [11] (2022) 101110.
  62. S.-B. Wang, P.-F. Zhao, X.-D. Jian, Y.-B. Yao, T. Tao, B. Liang and S.-G. Lu, “Large energy storage density and electrocaloric strength of Pb<sub>0.97</sub>La<sub>0.02</sub>(Zr<sub>0.46-x</sub>Sn<sub>0.54</sub>Ti<sub>x</sub>)O<sub>3</sub> antiferroelectric thick film ceramics”, *Scripta Mater.*, **210** (2022) 114426.
  63. R. Kumar, A. Kumar, S. Singh, “Coexistence of large negative and positive electrocaloric effects and energy storage performance in LiNbO<sub>3</sub> doped K<sub>0.5</sub>Na<sub>0.5</sub>NbO<sub>3</sub> nanocrystalline ceramics”, *ACS Appl. Electron. Mater.*, **1** [3] (2019) 454–460.